

Effect of Ca on structural and ferroelectric properties of $\text{SrBi}_2\text{Ta}_2\text{O}_9$ and $\text{SrBi}_2\text{Nb}_2\text{O}_9$ thin films

Rasmi R. Das, P. Bhattacharya, W. Pérez, Ram S. Katiyar*

Department of Physics, University of Puerto Rico, San Juan, PR 00931-3343, USA

Received 9 December 2003

Available online 27 April 2004

Abstract

In this study, we have improved the remanent polarization of $\text{SrBi}_2\text{Ta}_2\text{O}_9$ (SBT) and $\text{SrBi}_2\text{Nb}_2\text{O}_9$ (SBN) thin films using Ca substitution at Sr-site. SBT and SBN thin films with different concentrations of Ca were deposited on $\text{Pt/TiO}_2/\text{SiO}_2/\text{Si}$ substrates using pulsed-laser-deposition technique. The lattice parameters was found to be decreased with Ca incorporation and was attributed to the smaller ionic radii of Ca than for Sr. The modification in lattice vibrational frequencies with the incorporation of Ca in SBT and SBN films was investigated using micro-Raman spectroscopy. The grain size was increased with the increase in the Ca concentrations in SBT and SBN thin films. The SBT thin films with 20% Ca contents exhibited remnant polarization of $\sim 23.8 \mu\text{C}/\text{cm}^2$ with a coercive field of $\sim 175 \text{ kV}/\text{cm}$. The remanent polarization was found to be $\sim 35.5 \mu\text{C}/\text{cm}^2$ for SBN thin films with 10% Ca incorporation. The dielectric constant of SBT and SBN films was found to be decrease with Ca concentrations and observed to be independent of grain size.

© 2004 Elsevier Ltd and Techna Group S.r.l. All rights reserved.

Keywords: PLD; Ferroelectric; Bi-layered; SBT; SBN; Thin film

1. Introduction

Recently, ferroelectric thin films of $\text{SrBi}_2\text{Ta}_2\text{O}_9$ (SBT) and $\text{SrBi}_2\text{Nb}_2\text{O}_9$ (SBN), has been considered as a prime candidate materials for non-volatile random access memory (NVRAM) devices [1,2]. The fatigue free, low leakage current density, and fast switching characteristics of these materials are extremely useful for the reliable device operation. However, the low remanent polarization and higher crystallization temperature are the limiting factors for practical integration of SBT with Si processing technology. A large number of reports are intended to overcome these drawbacks by doping different concentration of cations at Sr, Ta-sites, or by growing off-stoichiometric SBT with excess Bi concentration [3–5]. Desu et al. [6] have reported the enhancement of remanent polarization in thin films with composition $(1-x)\text{SBT}-x\text{Bi}_3\text{Ti}(\text{TaNb})\text{O}_9$. Shimakawa et al. [7] calculated the effect of A-site cation on the electronic structure of SBT, on the basis of neutron diffraction data, and claimed that the substitution of smaller ionic radii cation (Ca) at the Sr-site of SBT caused pronounced lattice mismatch between

SrO and TaO_2 planes and led to higher value of spontaneous polarization. In practice, $\text{CaBi}_2\text{Ta}_2\text{O}_9$ (CBT) ferroelectric thin films showed poor ferroelectric properties than that of SBT [8,9]. In an earlier paper, we have reported the improved switching characteristics of SBT upon partial substitution of Sr by Ba and Ca [10]. Previously we have also studied the effect of growth conditions on the orientation of SBT and SBN thin films in order to achieve a high value of remanent polarizations [2,11,12]. In this article, we report a systematic structural and ferroelectric properties of Ca substituted SBT and SBN thin films. The change in microstructure with Ca substituted compositions of SBT and SBN thin films were correlated with the dielectric and ferroelectric properties.

2. Experimental

SBT and SBN thin films with various compositions, with different concentrations of Ca at Sr-site, were deposited on $\text{Pt/TiO}_2/\text{SiO}_2/\text{Si}$ substrates using pulsed-laser-deposition technique. Hereafter Ca substituted SBT and SBN represented by SCBT and SCBN. An excimer laser (KrF, 248 nm) with a laser energy density of $\sim 2.5 \text{ J}/\text{cm}^2$ and pulse repetition rate of 10 Hz was employed to grow thin films from the

* Corresponding author. Tel.: +1-787-764-4210;
fax: +1-787-764-2571.

E-mail address: rkatiyar@rrpac.upr.clu.edu (R.S. Katiyar).

dense ceramic targets. Thin films were deposited at a constant substrate temperature of 350 °C and oxygen pressure of 200 mTorr, followed by annealing at 750 °C for 1 h in oxygen ambient. The phase formation and crystalline quality of the films were identified using Siemens D5000 X-ray diffractometer, with Cu K α radiation. The surface morphology of the films was observed by atomic force microscopy (AFM, DI-Nanoscope IIIa). Platinum top electrodes of 200 μ m diameter and 200 nm thickness were deposited using DC magnetron sputtering. The ferroelectric hysteresis loops were measured using a ferroelectric tester (RT 6000 HVS, Radiant Tech.) at virtual ground mode. Fatigue characteristics were examined by using rectangular alternative pulses at 500 kHz and 150 kV/cm. The effect of Ca on the dielectric behavior of SBT thin films was studied by measuring the capacitance and tangential loss of the films at 100 kHz with an oscillating voltage of 100 mV.

3. Results and discussions

Bismuth layered ferroelectrics SBT and SBN have orthorhombic crystal structure with space group A2₁am at room temperature followed by tetragonal structure with space group I4/mmm in paraelectric phase [13]. The substitution or doping effects in Bi-layered structure is not straightforward as in the case of ABO₃ perovskites. The anisotropic characteristics in the crystal structure have a strong influence on the intrinsic electrical properties of these materials. The crystallization temperature of Aurivillius family of compounds has relatively higher value in comparison to lead based perovskites. The compositional dependent XRD patterns of SBT and SBN thin films with different concentrations of Ca were shown in Fig. 1. The films are polycrystalline in nature with the preferred orientation along the desired polarization axis (*a*–*b* plane). The relative intensity of (*I*₂₀₀/*I*₁₁₅) was found to be consistent irrespective of the Ca concentration in SBT films. It is clear from figure that the preferential orientation is significant in

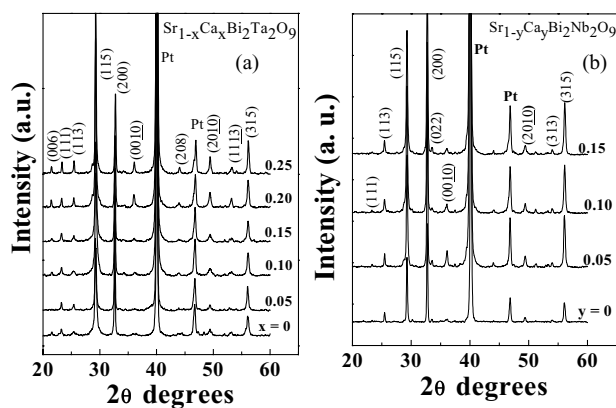


Fig. 1. XRD patterns of: (a) Sr_{1-x}Ca_xBi₂Ta₂O₉ and (b) Sr_{1-y}Ca_yBi₂Nb₂O₉ thin films.

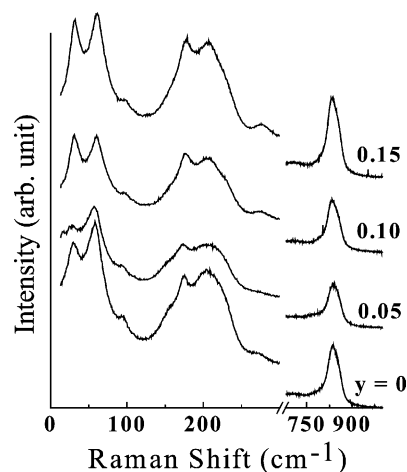


Fig. 2. Room temperature Raman spectra of Sr_{1-y}Ca_yBi₂Nb₂O₉ thin films.

case of Ca substituted SBN films in comparison to SBT. In an earlier report, we have shown that as-grown SBN films were preferentially oriented along the *c*-axis [11]. The orientation along *c*-axis is significantly suppressed by depositing amorphous thin films and annealing them at/above 700 °C. The diffraction peaks of SBT and SBN shifted towards higher diffraction angle with an incorporation of Ca at Sr-site, implied decrease in lattice parameter. This behavior could be attributed to the smaller ionic radii of Ca (1.36 Å) in comparison to Sr (1.43 Å). These lattice parameter variations are consistent with the reported results of Wu et al. [14]. There was no evidence of any fluorite or secondary phase formation after annealing at higher temperatures (~750 °C).

Raman spectroscopy was used to identify the influence of Ca in the lattice vibrational modes of SBT and SBN, and also confirming the occupying position of Ca by following the Raman active modes. Previously we have reported the influence of Ba and Nb substitution on the soft mode and O–Ta–O octahedral stretching mode of SBT ceramics and thin films [16]. Typical room temperature micro-Raman spectra of SCBN thin films grown at 350 °C and annealed at 750 °C are illustrated in Fig. 2. There was a small shift of the lowest transverse optic mode at 28.5 cm⁻¹ (*E_g* mode) towards higher wavenumber, upon incorporation of Ca. The A_{1g} Raman mode appeared at 61 cm⁻¹ also followed similar behavior. The observed data suggested that the transition temperature increases with the increase in Ca contents. The decrease in the tolerance factor and an increase in the soft mode frequency are consistent with the Raman spectra of previously observed Ca substituted SBT bulk and thin films [15,16]. The octahedral stretching mode observed at 834 cm⁻¹ is not affected by Ca substitution. The change in intensity of the O–Ta–O stretching mode could be attributed to the variation in the bond strength between various cations, since Ca has smaller ionic radii and smaller atomic mass than Sr.

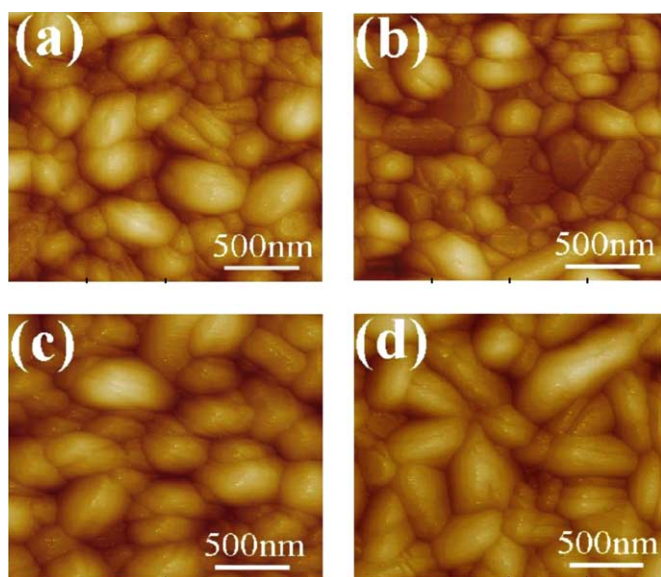


Fig. 3. AFM micrographs of $\text{Sr}_{1-y}\text{Ca}_y\text{Bi}_2\text{Nb}_2\text{O}_9$ thin films for different Ca concentrations (a) $y = 0$, (b) 0.05, (c) 0.1, and (d) 0.15.

The surface morphology of SCBT and SCBN thin films was observed using atomic force microscopy. Fig. 3 shows typical AFM micrographs of SCBN thin films after annealing at 750°C . It was clearly observed from the figure that the Ca has direct influence on the average grain size and homogeneity of the grains. The substitution of Ca gradually increases the grain size. The shape of SBN grains changes from oval to rod like structure at higher Ca contents. In case of SBN thin films larger grains of 550 nm was packed by smaller grains of 120 nm. The surface roughness of SBN thin films was found to be about 22 nm. With the increase in the Ca contents in SBN films led to the homogeneous distribution of the grains. The larger grain size was observed with the film having 15% Ca at Sr-site, in which rod like grains with the average length of grains of about 800 nm and width 300 nm are packed together. The root mean square surface roughness of the films was about 20–23 nm. Since the XRD figure shows the suppression of c -axis, this rod like grains can be considered as oriented grains along the polarization axis. The SBT thin films also showed increase in grain size and surface roughness with increasing Ca contents at Sr-site [17].

The ferroelectric properties of SBT and SBN layered perovskites are strongly orientation dependent due to large structural anisotropy in the lattice. The processing parameters played a crucial role in order to orient the films along the polarization axis. The tendency of growing the films along undesired c -axis and interdiffusion of bismuth with platinum electrode during high temperature processing are the major drawbacks of this family of compounds. In our earlier work, we have observed that bismuth-layered films, grown at higher substrate temperature, exhibited poor ferroelectric properties [11]. Whereas growth of amorphous films and annealed at higher substrate temperature led to

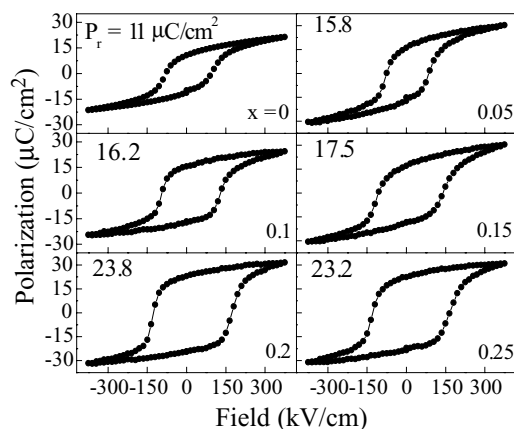


Fig. 4. Polarization-field hysteresis loops of $\text{Sr}_{1-x}\text{Ca}_x\text{Bi}_2\text{Ta}_2\text{O}_9$ thin films.

orient the grains along the polarization axis and showed enhanced ferroelectric properties [2,12]. The polarization-field hysteresis loops of SCBT thin films with different concentration of Ca are shown in Fig. 4. The maximum remanent polarization of SCBT thin films at 20% of Ca was found to be $23.8 \mu\text{C}/\text{cm}^2$ with coercive field of 170 kV/cm. The switching characteristics of SBT thin films improved upto certain concentration of Ca ($\sim 25\%$). The increase in polarization could be correlated to the pronounced structural distortion arises due to the partial substitution of smaller cation Ca at Sr-site. Another possible reason could be attributed to the increase in grain size of SBT, as observed in AFM micrographs. By substituting a smaller cation at A-site of bismuth layered perovskite reduced the value of the tolerance factor and this led to increase in the transition temperature and increase in the polarization values. Earlier, we have reported large polarization values of SBN thin films and were explained in terms of higher polarizability of Nb than Ta-ion [2]. The effective polarizability of the unit cell can also be improved by Ca incorporation in SBT, which resulted in to higher polarization values. However, the coercive field systematically increased with increase in Ca concentrations.

The SBN thin films showed a saturated hysteretic behavior with remanent polarization of $25.6 \mu\text{C}/\text{cm}^2$. With the increase in the Ca contents, it was observed that the polarization value gradually started increasing, as shown in Fig. 5. The SBN thin films with 10% Ca at Sr-site exhibited highest value of remanent polarization ($P_r \sim 35.5 \mu\text{C}/\text{cm}^2$). The coercive field was increased with increase in Ca contents. The increase in the polarization values could be due to the pronounced structural distortion inside the SrNb_2O_7 unit cell by the partial replacement of Ca or it could be attributed to the increase in the grain size. The increase in the coercive field might be due to the higher electronegativity of Ca. Fatigue was measured by applying bipolar pulses of 500 kHz at 7 V amplitude. The percentage of degradation of switchable polarization minus non-switchable polarization ($P^* - P'$) in SCBT and SCBN thin films was about $< 20\%$

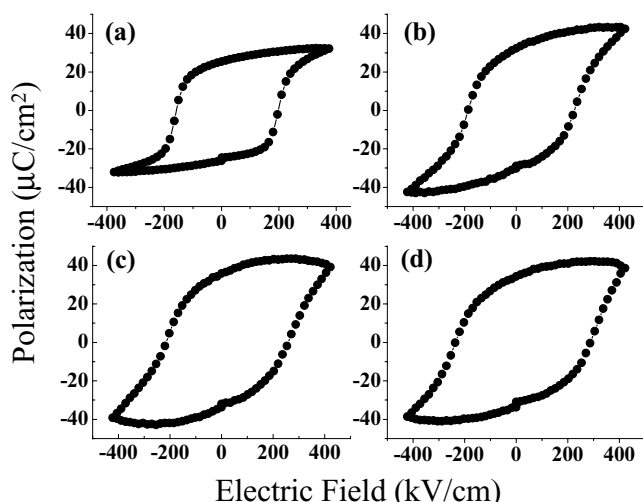


Fig. 5. Hysteresis loops of $\text{Sr}_{1-y}\text{Ca}_y\text{Bi}_2\text{Nb}_2\text{O}_9$ thin films at various Ca contents: (a) $y = 0$, (b) 0.05, (c) 0.1, and (d) 0.15.

after 10^{10} switching cycles, which makes it competitive for memory devices.

It is well known that the dielectric permittivity and tangential loss of ferroelectric thin films in most cases depended upon the composition, orientation, grain size and secondary phase, etc. Since bismuth layered perovskites are strongly anisotropic in nature, its dielectric behavior often influenced by the crystal structure. Fig. 6 shows the composition dependent dielectric permittivity and dissipation factor of SCBT thin films. Substitution of Ca in SBT thin films is a kind of solid solution of SBT and CBT systems. Since, the bulk dielectric constant of CBT is lower (~ 120) than SBT (~ 400), the effective dielectric constant of SCBT thin films decreased upon increase in Ca contents at Sr-site of SBT. The dissipation factor in this kind of ferroelectric thin films is originated from various sources such as domain wall pinning, interfacial diffusion between the film and bottom electrode, space charge accumulation at grain boundaries, oxygen vacancy, the presence of secondary phases, etc. It was noticed that the tangential loss of SCBT thin films did not show appreciable change with Ca incorporation. Fig. 7 shows the variation of

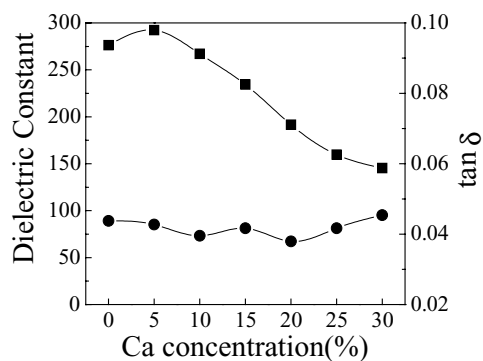


Fig. 6. Dielectric constant and tangential loss of SCBT thin film at different Ca concentrations.

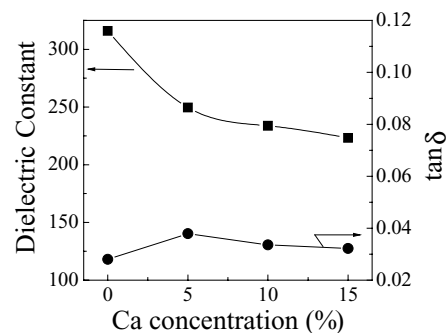


Fig. 7. Dielectric constant and tangential loss of SCBN thin film at different Ca concentrations.

dielectric constant and loss tangent of SBN thin films with different Ca concentrations. The dielectric constant was systematically decreased upon Ca incorporation in SBN. The substitution of Ca in SBN can be explained in the similar manner as of Ca in SBT. It is also known that $\text{CaBi}_2\text{Nb}_2\text{O}_9$ (CBN) has low value of dielectric permittivity, it might reduce the dielectric constant of SBN by the process of solid solution with SBN. The tangential loss of SCBN thin films was found to be similar magnitude as of Ca substituted SBT thin films. The increase in the grain size did not help to reduce the loss tangent of both SCBT and SCBN thin films.

4. Conclusion

In summary, SBT and SBN thin films with different Ca contents at Sr-sites were successfully grown using PLD technique. The in-plane lattice parameters of SBT and SBN were reduced by increasing Ca contents and was explained in terms of smaller ionic radii of Ca. The grain size and surface roughness of SBT and SBN films was observed to be increase with increasing Ca concentrations. The P_r values increased with increase in Ca contents, it was attributed to the pronounced structural distortion inside SrTa_2O_7 and SrNb_2O_7 perovskite units. SBT–20% Ca films exhibited P_r of $\sim 23.8 \mu\text{C}/\text{cm}^2$, whereas SBN–10% Ca films exhibited P_r of $\sim 35.5 \mu\text{C}/\text{cm}^2$, which is highest ever reported value. Dielectric permittivity of SBT and SBN thin films was reduced with increasing Ca concentrations and was attributed to the low permittivity nature of CBT and CBN systems.

Acknowledgements

This work was supported in parts by NASA-NCC5-518 and NSF-DMR-9801759 grants.

References

- [1] C.A. paz de Araujo, J.D. Cuchiaro, L.D. McMillan, M.C. Scott, J.F. Scott, *Nature* 374 (1995) 627.

- [2] R.R. Das, P. Bhattacharya, R.S. Katiyar, *Appl. Phys. Lett.* 81 (2002) 1672.
- [3] S.B. Desu, D.P. Vijay, *Mater. Sci. Eng. B* 32 (1995) 75.
- [4] R.R. Das, P. Bhattacharya, W. Perez, S. Katiyar, *J. Mater. Sci.* 38 (2003) 1171.
- [5] W. Lee, I. You, I. Yang, B. Yu, K. Cho, *Jpn. J. Appl. Phys.* 39 (2000) 5469.
- [6] S.B. Desu, P.C. Joshi, X. Zhang, S.O. Ryu, *Appl. Phys. Lett.* 71 (1997) 1041.
- [7] Y. Shimakawa, Y. Kubo, Y. Nakagawa, S. Goto, T. Kamiyama, H. Asano, F. Izumi, *Phys. Rev. B* 61 (2000) 6559.
- [8] R.R. Das, R.J. Rodriguez, R.S. Katiyar, S.B. Krupanidhi, *Appl. Phys. Lett.* 78 (2001) 2925.
- [9] K. Kato, K. Suzuki, K. Nishizawa, T. Miki, *J. Appl. Phys.* 89 (2001) 5088.
- [10] R.R. Das, P. Bhattacharya, W. Pérez, S. Katiyar, S.B. Desu, *Appl. Phys. Lett.* 80 (2002) 637.
- [11] R.R. Das, P.S. Dobal, A. Dixit, W. Pérez, M.S. Tomar, R.E. Melgar-ejo, R.S. Katiyar, *Mater. Res. Soc. Symp. Proc.* 655 (2001) CC5.6.1.
- [12] R.R. Das, P. Bhattacharya, W. Pérez, R.S. Katiyar, *Appl. Phys. Lett.* 81 (2002) 4052.
- [13] A.D. Rae, J.G. Thompson, R.L. Withers, *Acta Crystall. B* 48 (1992) 418.
- [14] Y. Wu, M.J. Forbess, S. Seraji, S.J. limmer, T.P. Chou, C. Nguyen, G. CaO, *J. Appl. Phys.* 90 (2001) 5296.
- [15] R.R. Das, W. Pérez, R.S. Katiyar, A.S. Bhalla, *J. Raman Spectrosc.* 33 (2002) 219.
- [16] W. Pérez, R.R. Das, P. Bhattacharya, R.S. Katiyar, *Integ. Ferroelec.* 42 (2000) 365.
- [17] R.R. Das, Ph.D. Thesis, 2003.